An optimized high-impedance amplifier for dry-electrode ECG recording

Cédric Assambo and Martin J. Burke

***Abstract*—**This paper presents the design, construction and performance verification of an ultra-low-power amplifier for use in long-term ambulatory recording of the human electrocardiogram (ECG) employing gel-free electrodes. The circuit structure has been optimized to provide the stringent low-frequency response characteristics and common-mode rejection ratio (CMRR) demanded in this application. The amplifier possesses a gain of 40 dB in a 3 dB bandwidth extending from 0.04 Hz to 1250 Hz. It also exhibits a maximum undershoot of 0.09 mV and a maximum recovery slope of 0.04 mVs^{-1} in response to a short 3mV input pulse of 100 ms duration, which is within the specification limits defined by international standards. The CMRR is greater than 95 dB at a mains frequency of 50 Hz. The amplifier draws a quiescent current of 15 μA from a 3 V battery, resulting in a total power consumption of less than 50 μW. Comparative *in-vivo* ECG recordings were obtained in several subjects at rest and under exercise conditions. The recordings obtained using the gel-free electrodes prove to be of equal quality to those obtained using traditional self-adhesive, gelled electrodes.

***Keywords*—**Dry-electrodes, electrocardiogram (ECG), high impedance, instrumentation amplifier.

I. Introduction

The ECG waveform is recorded from the surface of the skin using body electrodes and a recording amplifier. In conventional recording a coupling gel is used with the sensing electrodes, which must also be placed correctly on the subject's body by a professional medic. Many advances have been made in the quality and performance of disposable gelled or adhesive electrodes which are in everyday use. Nevertheless, some patients develop allergic reactions and skin irritation when these electrodes are used for long-term ambulatory recording of the ECG. Moreover, the gel also dries out over wearing time, which reduces signal quality and the performance of the recording system [1]. In more recent years, there has been a growing interest in the area of ambulatory ECG (AECG) recording using dry or ungelled electrodes for long term physiological monitoring [2] - [6]. The key advantage of dry electrodes is the elimination of allergic reactions commonly associated with electrolyte gels in long-term monitoring. Furthermore, the durability of dry electrodes over gel-based ones permits their shelf-life to be extended and their repeated reuse with proper disinfection.

The use of non-contact capacitive electrodes in the provision of non-intrusive ubiquitous ECG monitoring has been investigated [7] - [9]. Insulated electrodes having extremely low coupling capacitance require ultra-high input impedance amplifiers, which are highly susceptible to external electrostatic and electromagnetic interference even when shielding is used around the electrodes. Their reported lack of robustness has thus made insulated electrodes unsuitable for use with functional clothing [5]. Therefore, long-term ECG applications have generally employed dry, flexible, contact electrodes that rely on perspiration built on the surface of the skin to facilitate electrical conduction.

Much higher performance is required of the amplifier in the case of dry-electrode ECG monitoring than in conventional recording to compensate the lower electrical conductivity and their vastly different electrical properties. Optimized designs of the analog front-end amplifier have usually involved measuring the impedance of the skin-electrode interface. Some progress has been made in the realization of long-term telemetric ECG monitoring but the quality of signal recorded remains below that of a standard electrode Holter system [4]. Gargiulo et al. have presented an amplifier for dry-electrode ECG recording but without low-power in mind and thus it requires batteries to be recharged or changed regularly [3]. A micropower ECG amplifier exhibiting high CMRR performance and ultra-low noise characteristics was presented by Fay et al., but reference was not made to use with dry electrodes [10]. A previous design by Burke & Gleeson demonstrated the feasibility of dry-electrode ECG recording using a preamplifier that dissipates less than 30 μW of power [6]. However, performance requirements related to the system impulse response were not considered as they were not in operation at the time. Amplifier designs previously published are not readily adapted for use with the dry electrodes currently available. In this paper, the authors outline the design of a low-cost preamplifier employing commercially available components that is suitable for dry-electrode recording of the ECG, and provides a signal of adequate quality for clinical purposes in the light of the system performance requirements introduced in 2011 [11].

II. Essential Performance Requirements

Lack of fidelity in the reproduction of the ECG limits the ability of the cardiologist or an automated interpretation system to faithfully measure signal amplitudes, time relationships and waveform characteristics of the signal and may have serious clinical consequences. To ensure that the amplifier functions reliably in this regard, international standards dictate essential performance requirements. The International Electrotechnical Commission (IEC) is the

Both authors are with the Dept. of Electronic & Electrical Engineering, Printing House, Trinity College Dublin, Dublin 2, Rep. of Ireland.
Correspondence: Martin J. Burke; mburke@tcd.ie.

source of the majority of standards in electrocardiography applied world-wide [11], [12]. Despite the fact that standards in the USA are initially based on IEC documents, the American National Standards Institute (ANSI) generally considers recommendations of the American Heart Association (AHA) for its final texts [13] - [16].

A. Safe Current Limits

Specification limits related to patient safety relevant in low-voltage battery-powered applications in the range dc to the tenth harmonic of the power line frequency are listed in Table I. The more stringent requirement issued by the AHA is justified by studies reporting dangerous physiological changes occurring in patients connected to a 50 μA rms signal at 60 Hz over a 5 s period [16].

TABLE I
SAFE CURRENT LIMITS FLOWING THROUGH PATIENT

	AHA	ANSI & IEC
Max. current under normal condition	10 μA rms	10 μA rms
Max. current under fault condition	10 μA rms	50 μA rms

Inserting dc-blocking capacitors and current-limiting resistors in series with the sensing electrodes limits the current that can reach the patient's body. The dc-blocking capacitors have been placed in some amplifier designs in the second stage after moderate amplification but such a configuration allows op-amp bias currents to flow through the subject's body which can exceed the specified limit under fault conditions [17] - [19]. It also causes a voltage drop across the skin-electrode impedance, the magnitude of the latter being several MΩ at low frequency in the case of dry electrodes. This dc current can also charge the capacitance of the electrodes generating additional unwanted in-band artefact associated with motion and changes in the skin-electrode interface.

B. ECG Input Dynamic Range

The differential input signal range, its maximum rate of variation and the level of dc offset voltage specifications are given in Table II. If the preamplifier is to provide a 1 V ptp

TABLE II
DYNAMIC RANGE AND OFFSET VOLTAGE REQUIREMENTS

	Ambulatory ECG	Diagnostic quality ECG
Input range	±3 mV	±5 mV
Slew rate	125 mVs^{-1}	320 mVs^{-1}
Dc offset voltage	±300 mV	±300 mV

output to the subsequent signal conditioning stages, the required voltage gain in the frequency bandwidth of the signal must be 40 dB.

In addition, the maximum input signal rate of change must be considered for the selection of op-amps having sufficient slew-rate performance. Finally, the presence of a significant skin-electrode polarisation voltage confirms the need of dc-blocking capacitors in series with the dry contact electrodes. It should be noted that reduced dynamic range requirements are specified for AECG because it was assumed that AECG interpretations do not ordinarily involve analysis of the ECG features in fine morphological detail. However, the approach taken by the authors aims at designing an amplifier for diagnostic quality ECG recording, which implies adhering to the most stringent requirements.

C. Frequency Response

Frequency response requirements, summarised in Table III, must be considered at every stage of the design of an ECG amplifier. It has been proven that inadequate high-frequency response rounds off the sharp features of the ECG waveform and diminishes the amplitude of the QRS complex, while distortion in the slow varying detail such as the T wave occurs due to poor low-frequency performance, degrading the reproduction of the ST segment [20], [21]. Therefore, reproduction fidelity necessitates sufficient frequency bandwidth and a satisfactory phase characteristic to prevent signal distortion.

The AHA insists upon a 3-dB bandwidth of 0.05 – 250 Hz in AECG for infants weighing less than 10 kg and recommends that the amplitude response should be flat to within ±6% (±0.5 dB) over the range 0.14 to 30 Hz [14]. In addition, the AHA recommends that ECG amplifiers should introduce no more phase shift into the signal than that which is introduced by a 0.05-Hz, single-pole high-pass filter [14]. Our target 3-dB bandwidth has been extended to 0.05 - 2500 Hz in order to keep the phase shift introduced by the preamplifier below 6º within an ECG signal bandwidth of 0.5 - 250 Hz. More recently, low-frequency criteria have been specified in terms of the system impulse response. Both IEC and ANSI standards state that a 300 mVs impulse shall not yield an offset from the isoelectric line on the ECG record of greater than 0.1 mV, and shall not produce a recovery slope of greater than 0.3 mVs^{-1} following the end of the impulse [11] - [13]. The AHA recommends that a 1 mVs input impulse should not generate a displacement greater than 0.3 mV. The slope of the response outside the region of the impulse should nowhere exceed 1 mVs^{-1} [14], [15].

D. Optimizing Low-Frequency Performance

The amplifier front-end has been adapted to prevent the skin-electrode interface and the dc-blocking capacitors in series with the electrodes from giving rise to significant

TABLE III
FREQUENCY RESPONSE REQUIREMENTS

	AECG		Diagnostic quality ECG		
	AHA	ANSI & IEC	AHA	ANSI	IEC
Upper 3 dB cut-off freq.	60 Hz	55 Hz	250 Hz	150 Hz	40 Hz
Lower 3 dB cut-off freq.	0.05 Hz	0.05 Hz	0.05 Hz	0.67 Hz	0.67 Hz
Test input impulse width	1 mVs	0.3 mVs	1 mVs	0.3 mVs	0.3 mVs
Max. undershoot after impulse	0.3 mV	0.1 mV	0.3 mV	0.1 mV	0.1 mV
Max. recovery slope after impulse	1 mVs^{-1}	0.3 mVs^{-1}	1 mVs^{-1}	0.3 mVs^{-1}	0.3 mVs^{-1}

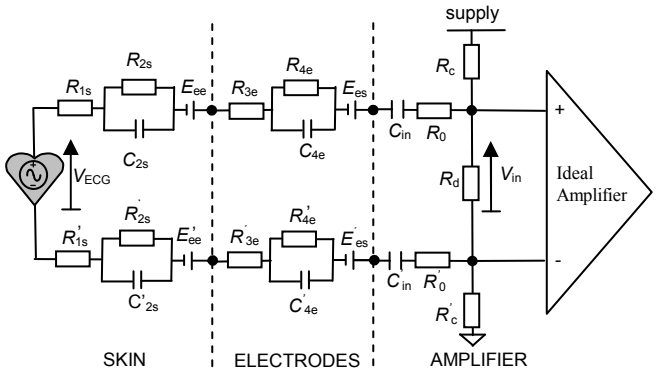

Fig. 1 Model of the Skin-Electrode-Amplifier Interface

low-frequency distortion of the ECG signal. A set-up showing the detection of an ECG signal from the body surface using a pair of sensing electrodes and a differential amplifier is schematically illustrated in Fig. 1. The common-mode input resistances, R_c and R_c', are the equivalent resistances of both inputs of the differential amplifier with respect to the analog common and the differential input resistance, R_d, is the equivalent resistance between the two inputs terminals. The overall input impedance $R_{in} = R_d//(2R_c)$ must be large enough to compensate the effective skin-to-electrode impedance over the frequency range of the signal and to guarantee that signals from all subjects will be monitored with the minimum attenuation and reproduction error.

The effect of the skin-electrode interface is simulated by means of a 620 kΩ resistor in parallel with a 4.7 nF capacitor in international standards. It is stated that at 10 Hz, the impedance of the combination should not cause an attenuation of greater than 20% in diagnostic quality ECG monitoring or 6% in AECG recording, leading to minimum values of amplifier input impedance as 2.5 MΩ and 10 MΩ, respectively.

The skin-electrode model shown in Fig. 1 was proposed by Kaczmarek & Webster [22]. It represents the skin-electrode interface as a double-time-constant system having one resistor-capacitor network associated with the skin-electrode contact and one associated with the epidermal layer of the skin itself. If R_c and R_d are taken as purely resistive, the frequency response of the combined skin-electrode-amplifier network as measured at the amplifier input is given as:

$$\frac{V_{in}(\omega)}{V_{ECG}(\omega)} = \frac{R_{in}}{R_{in} + 2\left(Z_e + R_0 + \frac{1}{j\omega C_{in}}\right)} \quad (1)$$

with the skin-electrode impedance Z_e given by:

$$Z_e = R_{1s} + R_{3e} + \frac{R_{2s}}{1 + j\omega R_{2s}C_{2s}} + \frac{R_{4e}}{1 + j\omega R_{4e}C_{4e}} \quad (2)$$

Baba & Burke developed a technique for measuring the impedance of the skin-electrode interface that relies upon the time response of the skin-electrode interface to a current pulse [23], [24]. Measurements were carried out on seven subjects, using several different types of dry electrodes, under variable conditions of contact pressure, electrode settling time and current level. The identification of the skin-electrode interface model parameters from 268 measurements returned values of resistance ranging from 640 Ω to 2.54 MΩ and of capacitance ranging from 0.1 μF to 432 μF, while values of the time constants $\tau_{2s} = R_{2s}C_{2s}$ and $\tau_{4e} = R_{4e}C_{4e}$ varied from 0.02 s to 31.29 s [23]. It can be shown that eq. (3) allows the amplitude response suggested by the AHA to be fulfilled while the phase response requirement is met by eq. (4):

$$R_{in} > 15.4\left(R_0 + R_{1s} + R_{3e} + \frac{R_{2s}}{1 + 39.5\tau_{2s}^2} + \frac{R_{4e}}{1 + 39.5\tau_{4e}^2}\right) \quad (3)$$

$$R_{in} \geq \frac{20}{\pi}\left(\frac{1}{C_{in}} + \frac{1}{C_{2s}} + \frac{1}{C_{4e}}\right) \quad (4)$$

For all measurements, the minimum input impedance that fulfils the amplitude response recommendation is 115 MΩ. Meeting the phase criterion requires a minimum input impedance of 750 MΩ.

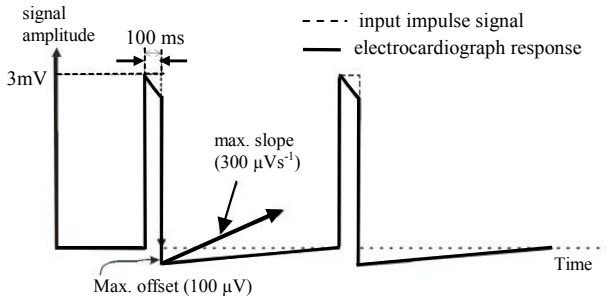

Fig. 2 A plot showing the time-domain specifications

An algorithm was developed in MATLAB to calculate the maximum undershoot and recovery slope for R_{in} values ranging between 10 MΩ and 10 GΩ and to find the minimum value for which the combined skin-electrode-amplifier network meets the impulse response requirements depicted in Fig. 2. The required minimum input impedance varies between 20 MΩ and 2 GΩ for a range of capacitance values of C_{in} varying from 0.01 μF to 3.3 μF, available in multilayer ceramic form. As suggested by eq. (4), it was observed that with increasing dc-blocking capacitance value, the parameters of the skin-electrode interface become the limiting factor [25]. All results confirm that meeting the impulse response specification requires the highest value of input impedance of 2GΩ, which was therefore selected as the target design value. This is seen to be well above the IEC specification value of 10 MΩ and highlights the shortcoming of this impedance specification for dry electrodes. The model parameter values of the skin-electrode interface associated with the highest input impedance requirement are: C_{2s} = 0.01 μF, C_{4e} = 0.1 μF, R_{2s} = 1.76 MΩ, R_{4e} = 1.84 MΩ and $R_{1s} + R_{3e}$ = 6 kΩ.

E. Optimizing CMRR performance

It is important to recognize that high fidelity in the reproduction of the ECG waveform requires a measurement system that preserves the ECG features and provides

amplification selective to the physiological signal while rejecting external interference and noise.

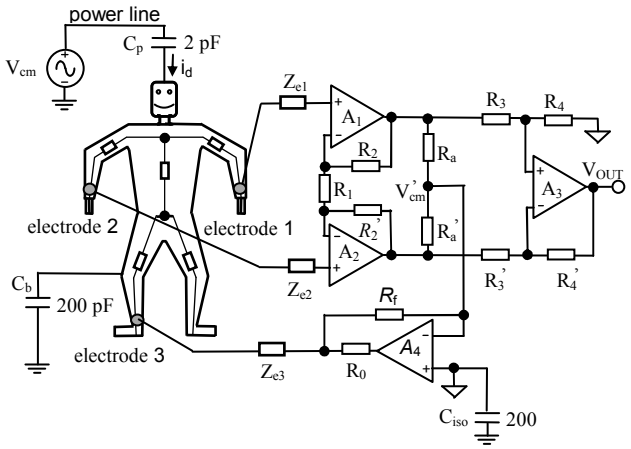

Fig.3 Schematic of ECG amplifier with right-leg-drive

As shown in Fig. 3, the electric field associated with the mains supply is capacitively coupled to the subject who is also coupled to ground via the body capacitance, C_b [26], [27]. With battery-operated instruments, when the common supply line of the amplifier is not at true earth potential, there is also an isolation capacitance, C_{iso}, present. A displacement current, i_d, then flows through the subject to ground, developing an interfering signal at the input to the recording amplifier. The CMRR of the amplifier is relied upon to suppress common-mode interference, and the performance requirements in this respect are listed in Table IV. There are three primary factors which contribute to the CMRR obtainable for the overall amplifier, namely: the component due to manufacturing tolerances in the gain-determining resistors, $CMRR_{\Delta R}$; the finite $CMRR_{op}$ of the op-amps used to implement the circuit; and the component due to common-mode impedance mismatch at the amplifier input, $CMRR_{\Delta Z}$. The overall CMRR of the amplifier is determined by the combination of these contributing factors as:

$$\frac{1}{\mathrm{CMRR}} = \frac{1}{\mathrm{CMRR}_{\Delta \mathrm{R}}} + \frac{1}{\mathrm{CMRR}_{\mathrm{op}}} + \frac{1}{\mathrm{CMRR}_{\Delta \mathrm{Z}}} \qquad (5)$$

The analog front-end amplifier shown in Fig. 3 is a standard circuit commonly used for biomedical signal sensing because it exhibits superior immunity to common-mode interference when compared to voltage follower and two-op-amp configurations. It can be shown that the minimum common-mode rejection ratio due to manufacturing tolerances $\pm\Delta_R$ in the gain-determining resistors is closely approximated by:

$$\mathrm{CMRR}_{\Delta \mathrm{R}} = \frac{\left(1+\frac{2R_2}{R_1}\right)\left(1+\frac{R_4}{R_3}\right)}{4\Delta_{\mathrm{R}}} = \left.\frac{A_{\mathrm{d}}}{2\Delta_{\mathrm{R}}}\right|_{R_3=R_4} \qquad (6)$$

where $A_d = (1+2R_2/R_1)(R_4/R_3)$ is the overall nominal differential gain of the amplifier. $CMRR_{\Delta R}$ is defined as the product of the CMRRs of the two individual amplification stages and is commonly approximated by $A_d/4\Delta_R$ [28] - [30]. Therefore the use of high gain in both stages of the circuit has been recommended for achieving high CMRR performance [6]. For a given nominal differential gain A_d, however, it can be shown that the differential gain should be allocated exclusively to the differential input stage whenever possible [31]. The gain of the differential-to-single-ended stage should thus be made unity by selecting $R_3 = R_4$. If a 1% manufacturing tolerance is assumed for all resistors and a differential mid-band gain of A_d = 40 dB is required, then in the worst-case scenario $CMRR_{\Delta R}$ = 74 dB.

TABLE IV
CMRR REQUIREMENTS

	AECG ANSI & IEC	Diagnostic quality ECG ANSI	Diagnostic quality ECG IEC
CMRR at mains freq.	60 dB	95 dB	89 dB
CMRR at 2xmains freq.	45 dB	N.A.	N.A.

The CMRR of an op-amp is defined as the ratio of its differential gain to its common-mode gain. Taking $CMRR_{op} >> 1$ and $R_3 = R_4$ in the circuit of Fig. 3, the Common-Mode Rejection Ratio due to the finite CMRR of the op-amps is closely approximated by:

$$\frac{1}{\mathrm{CMRR}_{\mathrm{op}}} = \frac{1}{\mathrm{CMRR}_{\mathrm{op1}}} + \frac{1}{\mathrm{CMRR}_{\mathrm{op2}}} + \frac{2}{A_{\mathrm{d}}\mathrm{CMRR}_{\mathrm{op3}}} \qquad (7)$$

The CMRR performance of suitable ultra-low-power op-amps commercially available allows the minimum $CMRR_{op}$ to be estimated at 64 dB.

Ideally, in the absence of a differential input signal, the voltages at the input terminals of the recording system are equal, resulting in V_{OUT} = 0 V at the output. However, imbalanced electrode impedances, Z_{e1} and Z_{e2}, and finite imbalanced values of common-mode input impedance, R_c and R_c' generate a differential signal at the input terminals of the op-amps from the common-mode input signal. Assuming a purely resistive input impedance, $CMRR_{\Delta Z}$ can be expressed in terms of the nominal impedances, Z_e and R_c, and their respective mismatch variations, Δ_e and Δ_c, as follows:

$$\mathrm{CMRR}_{\Delta \mathrm{Z}}\big|_{\mathrm{dB}} = 20\log_{10}\left(\frac{R_{\mathrm{c}}}{|Z_{\mathrm{e}}|}\right) + 20\log_{10}\left(\frac{1-\Delta_{\mathrm{c}}^2}{2\Delta_{\mathrm{c}}+2\Delta_{\mathrm{e}}}\right) \qquad (8)$$

The dominant variation in the impedances concerned is that of the skin-electrode interface, which if considered to be mismatched by a factor of 2:1 between electrodes, gives Δ_e = 0.33. The high design value of common-mode input impedance R_c = 2 GΩ with Δ_c = 0.03, coupled with the worst-case lowest electrode impedance magnitude $|Z_e|$ = 170 kΩ at 50 Hz yields a minimum value of $CMRR_{\Delta Z}$ of 85 dB. The overall CMRR of the differential amplification channel can then be evaluated using eq. (5) at $CMRR_{min}$ = 61 dB.

The effectiveness of right-leg body potential drivers in increasing the overall CMRR of instrumentation amplifiers has been demonstrated in ECG recording performed in a

three-electrode configuration, as shown in Fig. 3. Winter and Webster [27] showed that the common-mode signal on the body is reduced by the gain of the driven-right-leg circuit built around op-amp A_4 compared to that present without the right-leg-drive, which for the circuit shown is given as:

$$V_{\mathrm{cm}}^{'} = \frac{Z_{e3} i_d}{1 + \dfrac{2R_{\mathrm{f}}}{R_{\mathrm{a}}}} \tag{9}$$

F. Intrinsic noise vs power consumption

The target maximum level of noise at the output of the amplifier is 30 μV ptp when referred to the input, as stated in diagnostic quality ECG standards issued by both ANSI and IEC. This remains a challenging obstacle to the detection of low-level signals as noise performance is restricted in op-amps that are optimized for low supply voltage and ultra-low quiescent current. Semiconductor noise and its effect on signal-to-noise ratio in low-power dry-electrode ECG recording is analysed in more detail by Burke & Gleeson in [6]. It is desirable to use the lowest power op-amp available with suitable performance characteristics so that the power consumed by the recording amplifier can be minimised. Unfortunately, many manufacturers do not give sufficient information on the noise properties of their op-amps to allow accurate analysis to be carried out for their use in biomedical applications. As for all battery-powered equipment, an acceptable compromise must then be found between performance and power consumption. Equipment operating from a single voltage supply allows cost and circuit complexity to be reduced, since a single supply source can provide power to all components of the system. Low-cost 3 V lithium coin-cell batteries providing 1 Ah capacity are available today which can operate continuously for up to 30,000 h. Despite not being rechargeable, these batteries offer excellent shelf-life for their relatively small size and can support physiological monitoring over three to four years without a replacement of the battery.

III. Circuit Outline

Fig. 4 shows the circuit diagram of the ultra-low-power ECG amplifier proposed by the authors, optimized for enhanced CMRR and low-frequency performance. The difference between this and the design presented by Burke & Gleeson [6] resides essentially in the distribution of the gain within the amplification channel and the redesign of characteristics. In this revised structure the differential gain has been exclusively allocated to the second fully differential amplification stage built around op-amps A_3 and A_4. The front-end in this design acts as an impedance defining unity-gain buffer stage. The use of unity gain here allows the effects of mismatch of gain-determining resistors used in earlier versions of the circuit to be eliminated [6], [32], [33]. Input bias currents are prevented from reaching the patient's body by the coupling capacitors C_{0A}, C_{0B} and C_{0C}. Therefore, the dc-current that flows from the power supply to the analog common rail finds its path through resistors R_{2A}, R_3 and R_{2B} in series. These resistors also define the dc bias voltages at the input terminals of op-amps A_1 and A_2 at $3V_{\mathrm{cc}}/4$ and $V_{\mathrm{cc}}/4$, respectively. This is achieved by selecting $R_{2A} = R_{2B} = R_2 = R_3/2$. The dc bias voltages are preserved on each side of the second differential stage by ensuring that the dc gain is unity with the use of capacitor, C_1. The use of unity gain in the differential-to-single-ended output stage results in an output dc bias voltage equal to $V_{\mathrm{cc}}/2$. The use of unity gain in the final stage also aids in maximizing the overall CMRR. Because the two op-amps of the second stage provide the differential gain for the circuit, it is crucial that their gain-bandwidth products are sufficiently large to secure amplification of the input signal without amplitude or phase distortion within the ECG bandwidth. Op-amps from the MAX9910 series (Maxim Inc.) were used for this purpose. The two unity-gain stages at the front-end and at the output are built around op-amps from the OPA369 series (Analog Devices Inc.) for which the frequency characteristics exceed the bandwidth of interest. All five op-amps in the differential amplification channel are unity-gain stable.

Low cost 1% tolerance resistors are currently available in surface mount form for resistance values up 20 MΩ, which is the value used for R_{1A} and R_{1B}. The lower ends of these resistors are connected to either side of resistor R_3 which receives positive feedback from the outputs of op-amps A_1 and A_2 via resistors R_{2A} and R_{2B} respectively. This bootstrapping mechanism allows the magnitude of the currents flowing across R_{1A} and R_{1B} to be reduced, making their resistance appear much higher at the amplifier inputs [6]. Selecting $R_{1A} = R_{1B} = R_1$, $R_{4A} = R_{4B} = R_{4B}$ and $R_1 >> R_2$ allows the input impedance characteristics of the circuit to be closely approximated by:

$$R_{\mathrm{d}} \approx R_1 \left[2 + \frac{R_3 (R_2 + R_4)}{R_2 R_4} \right] \left(1 + \frac{R_4}{R_2} \right) \approx 4.31\,\mathrm{G\Omega} \tag{10}$$

$$R_{\mathrm{c}} \approx R_1 \left(1 + \frac{R_2}{R_4} \right) \approx 2.02\,\mathrm{G\Omega} \tag{11}$$

with

$$\Delta_{\mathrm{c}} \approx \frac{R_4}{R_2 + R_4} \left[1 + \frac{R_2}{R_4} \left[\frac{2R_4^2 + 3R_3 (R_2 + R_4)}{2R_2 R_4 + R_3 (R_2 + R_4)} \right] \right] \Delta_{\mathrm{R}} \approx 2.95\% \tag{12}$$

A mid-band gain of 40 dB is obtained with $R_{7A} = R_{7B} = R_7 =$ 10 MΩ and $R_6 = 200$ kΩ. Capacitances C_{4A}, C_{4B}, C_{5A} and C_{5B} have been included to prevent the risk of instability that may be caused by parasitic capacitances at the input of op-amps A_3 and A_4. The amplifier frequency response is preserved by using pole-zero cancellation in making $2C_{5A}R_{7A} = 2C_{5B}R_{7B} = C_{4A}R_6 = C_{4B}R_6$ [6]. Choosing $C_{4A} = C_{4B} = C_4 = 100$ pF overcomes the effect of variation in the input capacitance of the op-amps and creates a zero at 16 kHz which is cancelled by the pole created by selecting $C_{5A} = C_{5B} = C_5 = 1$ pF. The transfer function of the amplifier circuit is then given by:

$$\frac{V_{\mathrm{OUT}}(s)}{V_1(s) - V_2(s)} = \left(1 + \frac{2R_7}{R_6} \right) \left(\frac{s}{s + 2\pi f_{\mathrm{c1}}} \right) \left(\frac{s + \dfrac{2\pi f_{\mathrm{c2}}}{1 + 2\mathrm{R}_7/\mathrm{R}_6}}{\mathrm{s} + 2\pi f_{\mathrm{c2}}} \right) \tag{13}$$

where $f_{\mathrm{c1}} = 1/(\pi R_{\mathrm{in}} C_0)$, $f_{\mathrm{c2}} = 1/(2\pi R_6 C_1)$ and C_0 is the

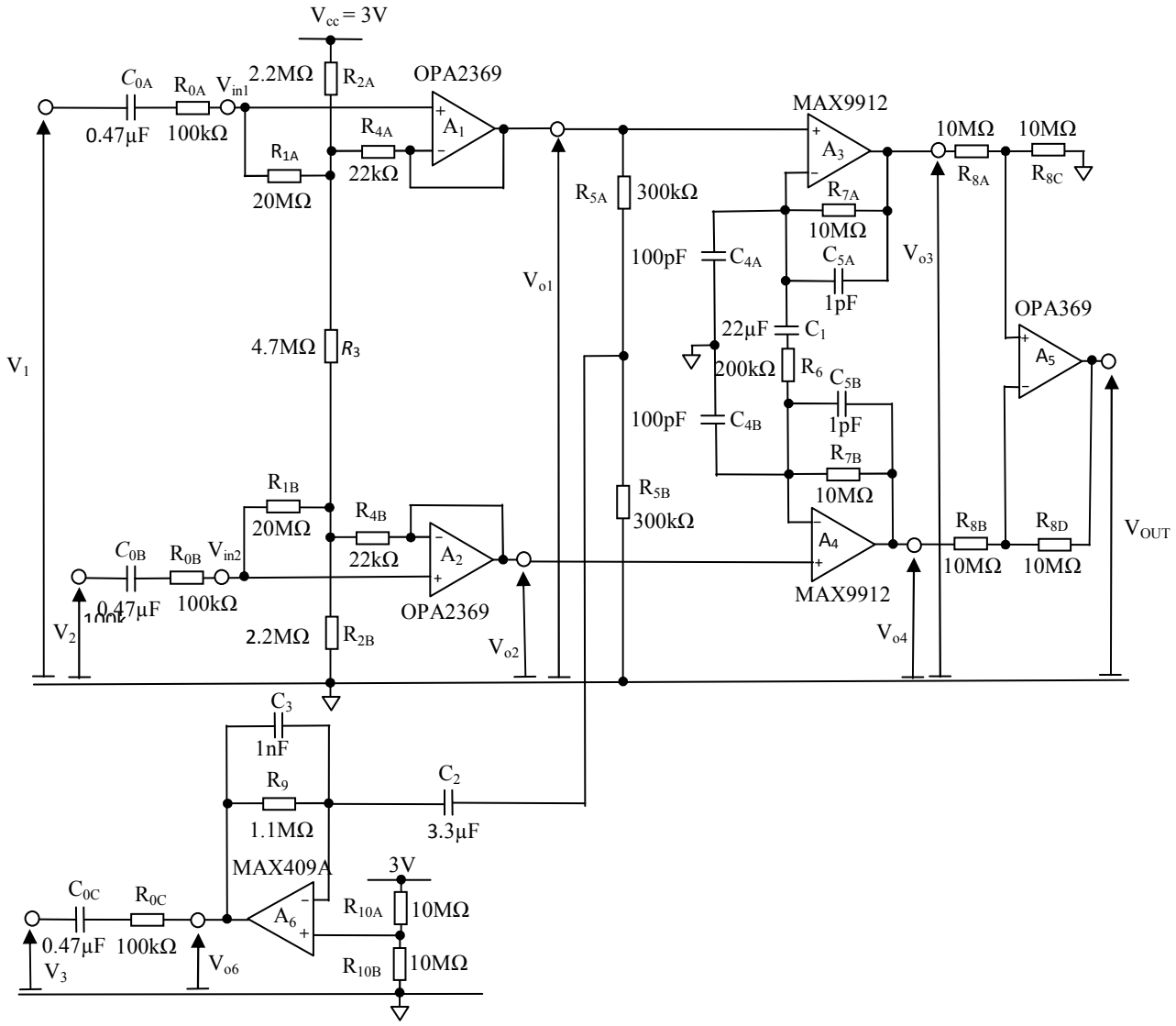

Fig. 4 Schematic diagram of the optimized low-power dry-electrode ECG recorindg amplifier

capacitance of the dc-blocking capacitors C_{0A} and C_{0B}. Selecting C_1 = 22 μF sets the low-frequency cutoff f_{c2} at 0.036 Hz, fulfilling the AHA recommendations listed in Table III. In addition, the combined response of the first and second stages are made equivalent to that of a single-pole high-pass filter by making $f_{c1} = f_{c2}/(1+R_7/R_6)$. This is achieved with C_0 = 0.47 μF, leading to a simplified transfer given by:

$$\frac{V_{OUT}(s)}{V_1(s)-V_2(s)} = \left(1+\frac{2R_7}{R_6}\right)\left(\frac{R_6C_1s}{1+R_6C_1s}\right) \tag{14}$$

CMRR performance is enhanced by the implementation of a common-mode right-leg drive feedback circuit built around op-amp A_6. The transfer function of this stage is given as:

$$\frac{V_{o6}(s)}{0.5\left(V_{o1}(s)+V_{o2}(s)\right)} = -\frac{2R_9}{R_5}\frac{(R_5/2)C_2s}{(1+R_9C_3s)[1+(R_5/2)C_2s]} \tag{15}$$

Instability was experienced during actual ECG recording when the gain of driven-right-leg circuit was set relatively high, at around 40 dB. The problem was solved by reducing the gain to a maximum of 17 dB in the 3dB bandwidth 0.3 – 100 Hz.

IV. Performance Evaluation

The proposed ECG amplifier circuit was first simulated in PSpice to allow the predicted performance to be verified before a prototype was built and tested. Bench test results confirm that the measured response is in accordance with simulation results at low frequencies, fulfilling the performance requirements. However, discrepancies between theoretical and measurement responses at high frequency were observed. This is believed to be caused by the presence of parasitic capacitance on the circuit board not accounted for in the circuit model. Plots of the differential amplitude and phase responses are shown in Figs. 5 and 6, respectively. The 3-dB bandwidth of the amplifier extends from 0.04 Hz to 1.25 kHz and the phase shift introduced is within ±6º from 0.38 Hz to 98 Hz.

The impulse response was tested with an input pulse of 3 mV in amplitude and 100 ms in duration repeated every 2 s. The maximum undershoot and the maximum recovery slope at the end of the impulse were measured at 0.09 mV and

0.04 mVs^{-1}, respectively, referred to the input. These values are within the specification limits given in Table III.

Input impedance and CMRR characteristics were measured in the frequency range 0.5 Hz – 10 kHz. At the lower end of the ECG spectrum, 0.5 Hz, the amplifier input impedance $R_{in} = R_d//(2R_c)$ was measured as 2.1 GΩ and the CMRR as 108 dB. At mains frequency, 50 Hz, the common-mode input impedance R_c was measured as 2.2 GΩ and the CMRR as 97 dB. The CMRR at twice the mains frequency was 89 dB. Input impedance and CMRR requirements are therefore met.

The level of output noise was evaluated for both wet and dry electrodes connected together and individually to the analog common rail. Noise was measured in all cases at 200 μV ptp, when referred to the input. This suggests that the output noise level is not noticeably affected by the presence of the input electrodes and can be considered to be semiconductor noise generated within the op-amps. Results of the bench tests are summarized in Table V below.

TABLE V
SUMMARY OF TEST RESULTS

	Measurement	Target value
Supply voltage	3 V	3 V
Power	45 μW	50 μW (max)
Gain	40 dB	40 dB
3dB Bandwidth	0.04 – 1250 Hz	0.05 – 2500 Hz
±0.5 dB Bandwidth	0.1 – 45.4 Hz	0.14 – 30 Hz
Phase at 0.5 Hz	4.6º	6º (max)
CMRR at 50 Hz	97 dB	95 dB (min)
Max. undershoot	0.09 mV	0.1 mV
Max. slope	0.04 mVs^{-1}	0.3 mVs^{-1}
Noise ref. to input	200 μV	30 μV (max)

Fourteen healthy volunteers, 10 male and 4 female, aged between 22 and 41 years were recruited for the recording of *in-vivo* ECG signals using standard Ag/AgCl pre-gelled electrodes (Schiller Biotabs, 2.3 x 2.3 cm) and conductive silicon rubber dry electrodes (Pro Carbon C5005PF, 2.6 cm diameter). The dry electrodes were disinfected with an alcohol wipe before being applied to the skin, but the skin was not cleaned, abraded or prepared in any way.

A sample ECG waveform recorded from one subject while standing at rest is shown in Fig. 7 and while the subject was undergoing the Harvard step test in Fig. 8. The quality of the recorded lead II ECG waveforms is comparable for measurements taken with dry and wet electrodes for both resting and exercising condition. Baseline variation and motion artefact can be observed in tracings recorded during exercise but is not any worse using dry electrodes compared with adhesive jelled electrodes. The exercise recordings in both cases clearly need further processing before being useful for clinical purposes.

Semiconductor noise affects all waveforms but does not seriously degrade the recorded signal. Nonetheless, the level of noise present is higher than that allowed by international standards. This can be reduced by using better quality op-amps with lower noise characteristics but this will be at the expense of higher quiescent currents and hence increased power consumption.

V. CONCLUSION

The design of the optimized low-power dry-electrode ECG amplifier reported by the authors has concentrated on essential performance requirements recently introduced. An earlier design published by Burke & Gleeson in 2000 presented a circuit structure suitable for dry-electrodes applications. The revised and optimized circuit presented exhibits enhanced low-frequency and CMRR performance compared with previous versions [6], [32], [33]. The power consumption of the circuit presented is very low at only 45 μW when operating form a 3V battery, making the amplifier ideally suited to long-term ambulatory ECG monitoring. Reducing semiconductor noise will require the use of op-amps with higher quiescent currents, and consequently higher power consumption.

The effect of baseline wander and motion artefact is expected to be reduced by having a complete recording system integrated in a body-fit vest, securing good contact between skin and electrodes and preventing the movement of leads.

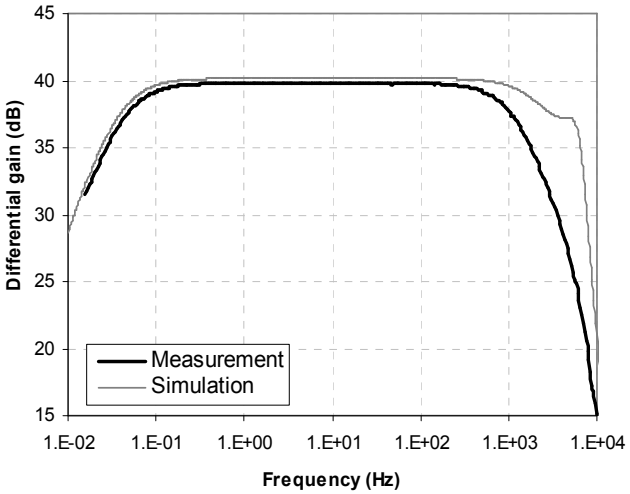

Fig. 5. Measurement plots of the amplitude response compared with simulation results.

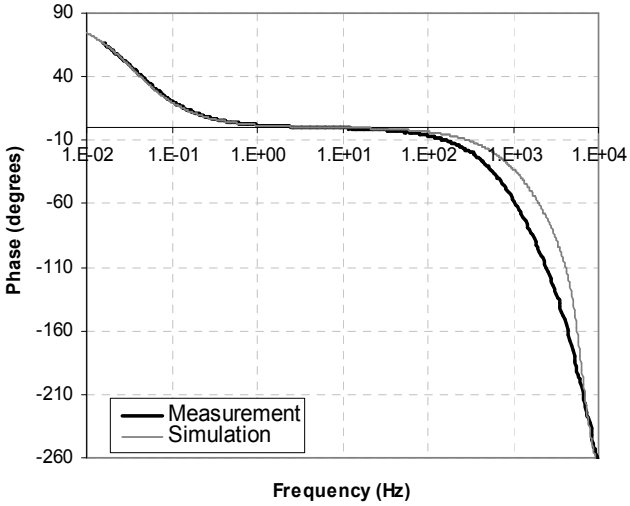

Fig. 6. Measurement plots of the phase response compared with simulation results.

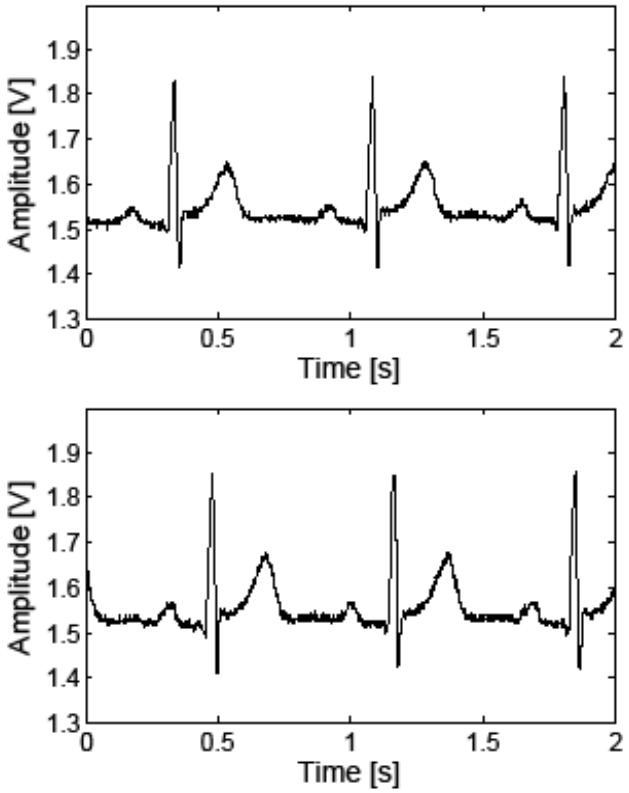

Fig. 7. Sample resting ECG recordings using dry electrodes (upper trace) and wet electrodes (upper trace).

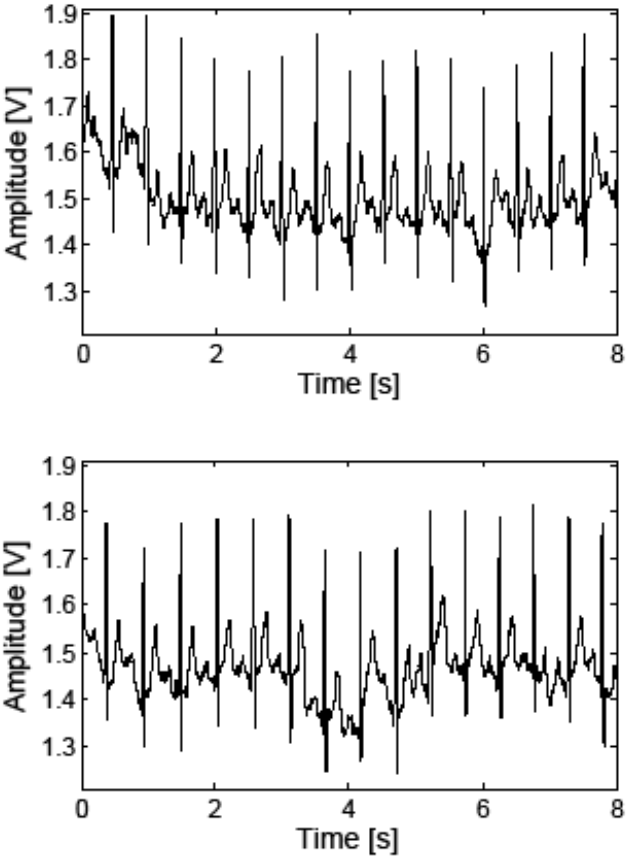

Fig. 8. Sample ECG recordings measured with subject undergoing a Harvard step test using dry electrodes (upper trace) and wet electrodes (lower trace).

REFERENCES

[1] A. Searle and L. Kirkup, "A direct comparison of wet, dry and insulating bioelectric recording electrodes," *Physiol, Meas.*, vol. 21, no. 2, May 2000, pp. 271-283.

[2] C. L. Chang et al., "A power-efficient bio-potential acquisition device with ds-mde sensors for long-term healthcare monitoring applications," *Sensors*, vol. 10, May 2010, pp. 4778-4793.

[3] G. Gargiulo et al., "An ultra-high input impedance ecg amplifer for long-term monitoring of athletes," *Med. Dev. Evid. Res.*, vol. 2010-3, July 2010, pp. 1-9.

[4] S. Fuhrhop et al., "Ambulant ecg recording with wet and dry electrodes: A direct comparison of two systems," in *IFMBE Proc*, vol. 25 / V, Munich, 2009, pp. 305-307.

[5] J. Mühlstef and O. Such, "Dry electrodes for monitoring of vital signs in functional textiles," in *Conf. Proc. IEEE Eng. Med. Biol. Soc.*, San Francisco, Sept. 2004, pp. 2212-2215.

[6] M. J. Burke and D. T. Gleeson, "A micropower dry-electrode ecg preamplifer," *IEEE Trans. Biomed. Eng.*, vol. 47, Feb. 2000, pp. 155-162.

[7] Y. G. Lim et al., "Monitoring physiological signals using nonintrusive sensors installed in daily life equipment," *Biomed. Eng. Lett.*, vol. 1, Feb. 2011, pp. 11-20.

[8] H. J. Baek, J. S. Kim, K. K. Kim, and K. S. Park, "System for unconstrained ecg measurement on a toilet seat using capacitive coupled electrodes : The efficacy and practicality," *Conf. Proc. IEEE Eng. Med. Biol. Soc.*, Vancouver, Aug. 2008, pp. 2326-2328.

[9] E. Spinelli and M. Haberman, "Insulating electrodes: a review on biopotential front ends for dielectric skin electrode interfaces," *Physiol. Meas.*, vol. 31, Sept. 2010, pp. S183-S198.

[10] Fay, L., V. Misra, and R. Sarpeshkar. "A Micropower Electrocardiogram Amplifier." *IEEE Trans. Biomed. Circuits Syst.*, vol. 3, May 2009, pp. 312-320.

[11] International Electrotechnical Commission, 'Medical electrical equipment Part 2-27: Particular requirements for the safety, including essential performance, of electrocardiographic monitoring equipment', IEC Std. IEC60 601-2-27:2011, 3rd ed., March 2011.

[12] International Electrotechnical Commission, 'Medical electrical equipment Part 2-47: Particular requirements for the safety, including essential performance, of ambulatory electrocardiographic systems, IEC Std. IEC60 601- 2-47:2001, ed. 1, July 2001.

[13] American National Standards Institute, 'Diagnostic electrocardiographic devices, AAMI Std. ANSI/AAMI EC11:1991/(R)2001/(R)2007, Aug. 2007.

[14] P. Kligfield et al., "Recommendations for the standardization and interpretation of the electrocardiogram: Part I: The electrocardiogram and its technology: A scientific statement from the American heart association electrocardiography and arrhythmias committee, council on clinical cardiology; the American college of cardiology foundation; and the heart rhythm society endorsed by the international society for computerized electrocardiology," *Circulation*, vol. 115, March 2007, pp. 1306-1324.

[15] L. T. Sheffield et al., "AHA special reports: Recommendations for standards of instrumentation and practice in the use of ambulatory electrocardiography," *Circulation*, vol. 71, March 1985, pp. 626A-636A.

[16] M. Laks et al., "Recommendations for safe current limits for electrocardiographs, "*Circulation*, vol. 93, 1996, pp. 837-839.

[17] E. M. Spinelli, N. Martinez, M. A. Mayosky, and R. Pallás-Areny, "A novel fully differential biopotential amplifier with dc suppression," *IEEE Trans. Biomed. Eng.*, vol. 51, Aug. 2004, pp. 1444-1448.

[18] E. M. Spinelli, R. Pallás-Areny, and M. A. Mayosky, "Ac-coupled front-end for biopotential measurements," *IEEE Trans. Biomed. Eng.*, vol. 50, March 2003, pp. 391-395.

[19] E. M. Spinelli, N. H. Martinez, and M. A. Mayosky, "A single supply biopotential amplifier," *Med. Eng. Phys.*, vol. 23, April, pp. 235-238.

[20] A. S. Berson and H. V. Pipberger, "The low frequency response of electrocardiographs, a frequent source of recording errors," *Amer. Heart J.*, vol. 71, no. 6, July 1996, pp. 779-789.

[21] D. Tayler and R. Vincent, "Signal distortion in the electrocardiogram due to inadequate phase response," *IEEE Trans. Biomed. Eng.*, vol. 30, no. 6, June 1983, pp. 352-356.

[22] K. A. Kaczmarek and J. G. Webster, "Voltage-current characteristics of the electrotactile skin-electrode interface," in *Conf. Proc. IEEE Eng. Med. Biol. Soc.*, vol. 5, Seattle, 1989, pp. 1526-1527.

[23] A. Baba and M. J. Burke, "Electrical characterisation of dry electrodes for ecg recording," *Proc. 12th WSEAS Int, Conf. Circuits*, Crete, July 2008, paper 591-226.

[24] A. Baba and M. J. Burke, 'Measurement of the electrical characteristics of ungelled ECG electrodes.' *NAUN Int. J. Biol. Biomed. Eng.*, vol. 2, no. 3, 2008, pp. 89-97.

[25] C. Assambo and M. J. Burke, "Amplifier input impedance in dry electrode ecg recording," in *Conf. Proc. IEEE Eng. Med. Biol. Soc.*, Minneapolis, Sept. 2009, pp. 1774-1777.

[26] M. R. Neuman, 'Biopotential Amplifiers', in *Medical instrumentation*; 3rd ed., J. G. Webster (ed.), Wiley, 1998, ch. 6, pp. 289-353.

[27] B. Winter and J. G. Webster, "Driven-right-leg circuit design," *IEEE Trans. Biomed. Eng.*, vol. 30, Jan. 1983, pp. 62-66.

[28] R. Pallás-Areny and J. G. Webster, *Analog signal processing*. John Wiley & Sons, 1999.

[29] R. Pallás-Areny and J. G. Webster, "Common mode rejection ratio for cascaded differential amplifier stages," *IEEE Trans. Instrum. Meas.*, vol. 40, Aug. 1991, pp. 677-681.

[30] M. Smither, D. Pugh, and L. Woolard, "C.M.R.R. analysis of the 3-op-amp instrumentation amplifier," *Electronics Lett.*, vol. 13, Sept. 1977, p. 594.

[31] C. Assambo, 'Amplifier Front-end design in dry-electrode electrocardiography.' PhD Thesis, Dept. Electronic and Electrical Engineering, Trinity College, Dublin 2, Rep. of Ireland, June 2011.

[32] Burke, M. J. and Assambo, C., 'An improved micro-power pre-amplifier for dry-electrode ECG recording', *Proc. 11th WSEAS Int. Conf. Circuits*, Crete, July 2007, paper 561-286.

[33] C. Assambo and M. J. Burke, 'An Improved very-low power pre-amplifier for use with un-gelled electrodes in ECG recording', *NAUN J. Biol. Biomed. Eng.*, vol. 1, no. 1, 2007, pp. 25-35.